Supplementary Information for

Simultaneous regeneration of epithelial and bone tissue using a multifunctional film with leaf-stacked structure and growth factors

Ho Yong Kim[†a], Han Byul Kim[†a], Jin-Ho Park[b,c], Min Ji Kim[a], June-Ho Byun[*d], and Se Heang Oh[*a,e]

[a]*Department of Nanobiomedical Science, Dankook University, Cheonan, 31116, Republic of Korea*

[b]*Department of Biology, College of Natural Science, Kyungpook National University, Daegu, 41566, Republic of Korea*

[c]*School of Life Sciences, BK21 plus KNU Creative BioResearch Group, Kyungpook National University, Daegu, 41566, Republic of Korea*

[d]*Department of Oral and Maxillofacial Surgery, Gyeongsang National University School of Medicine, Gyeongsang National University Hospital, Institute of Health Science, Gyeongsang National University, Jinju, 52828, Republic of Korea*

[e]*Department of Biomedical Sciences & Biosystems, Dankook University, Cheonan, 31116, Republic of Korea*

†These authors contributed equally to this work.

*Corresponding authors.

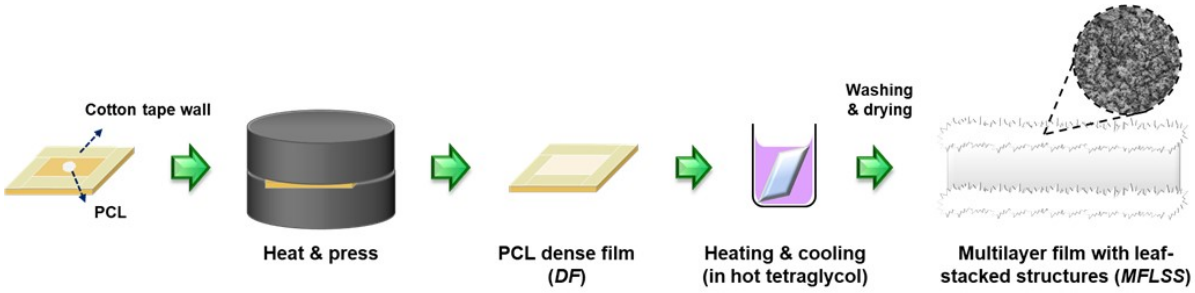

Fig. S1. Schematic diagram depicting the fabrication process of the multilayer film featuring leaf-stacked structures (*MFLSS*).

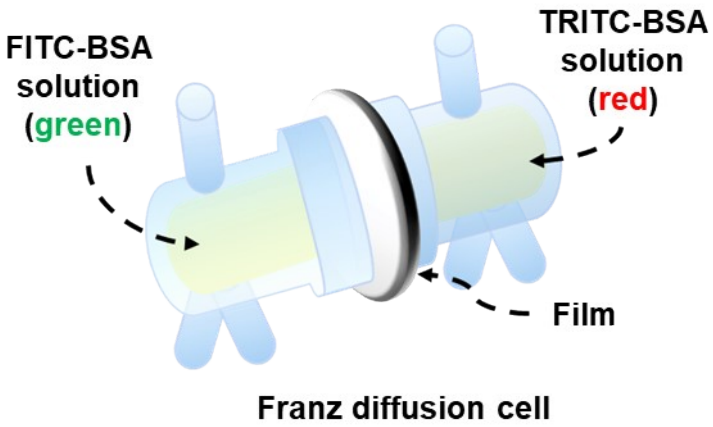

Fig. S2. Schematic diagram illustrating the procedure for loading proteins or growth factors onto the films (*DF* or *MFLSS*) using Franz diffusion cells.

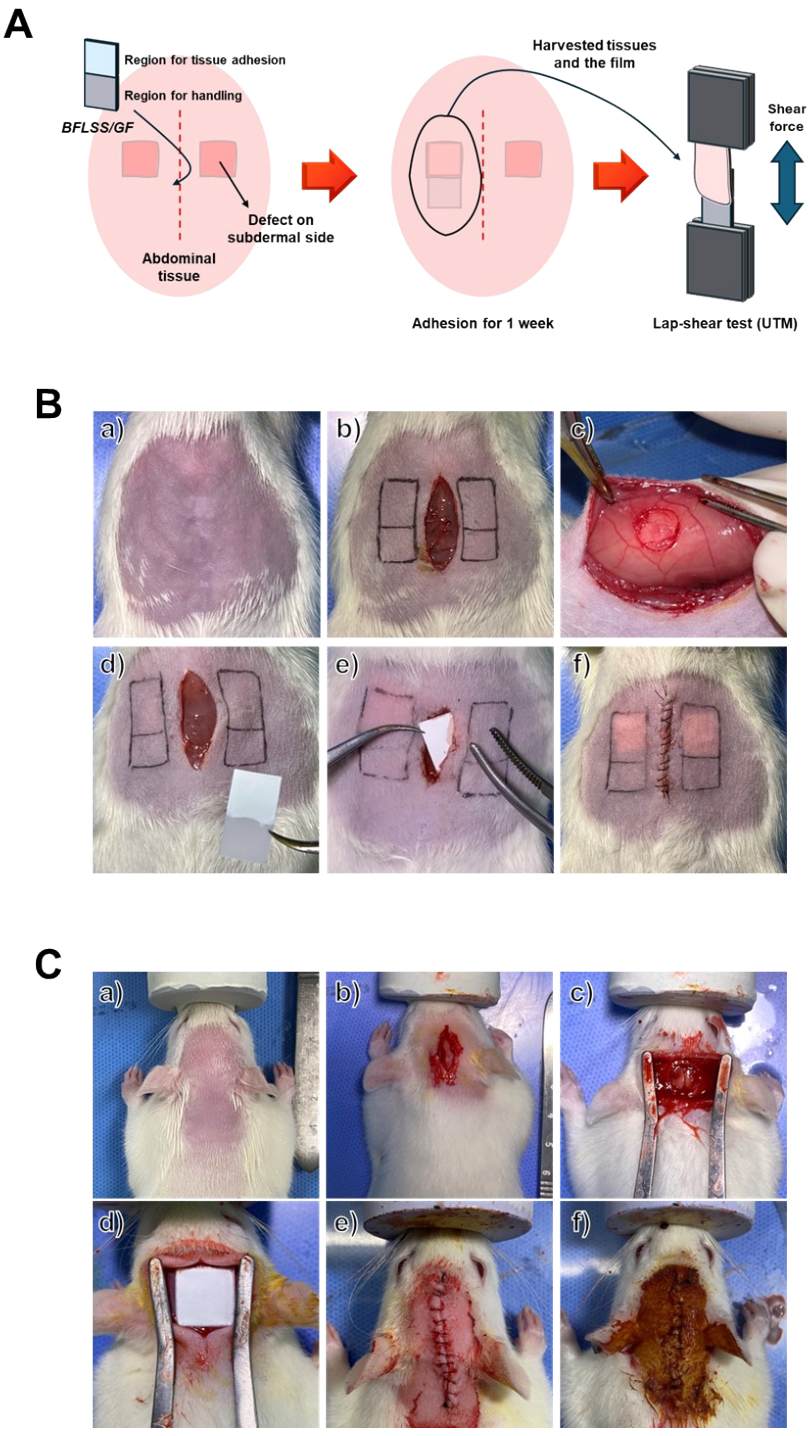

Fig. S3. (A) Schematic depiction of the *MFLSS/PDGF* used for the rat epithelium adhesion model and mechanical strength analysis (lap-shear test). (B) Overview of the rat epithelium adhesion model protocol and (C) experimental design for the rat calvarial defect model.

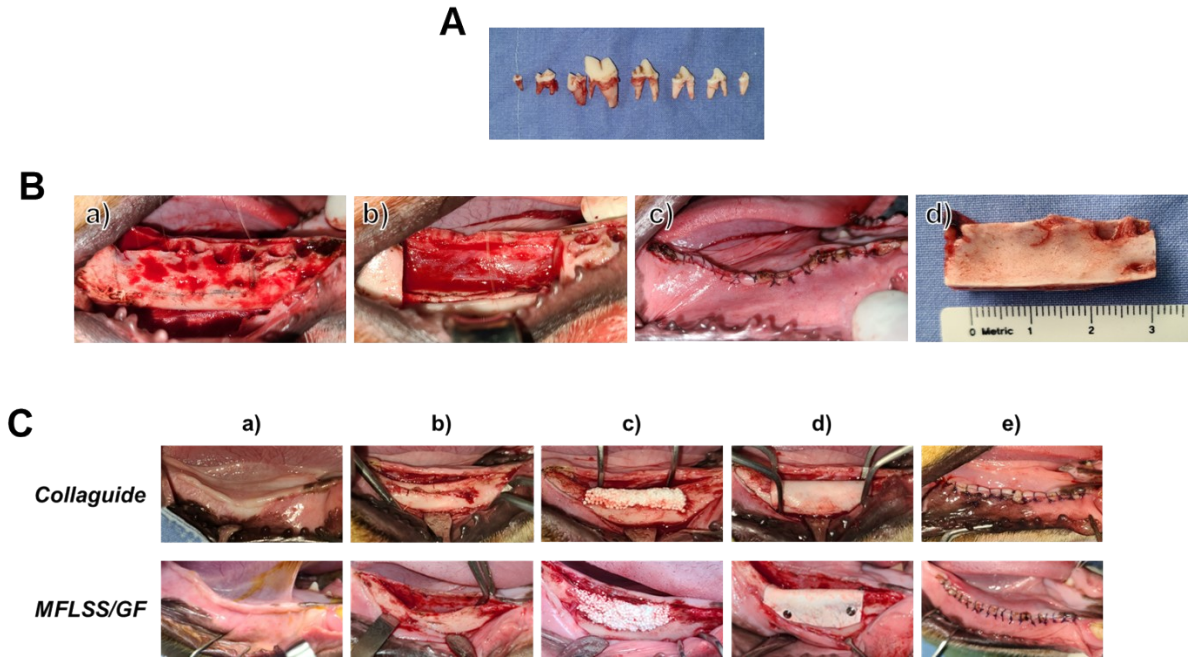

Fig. S4. Representative animal model setup and surgical procedures for *Collaguide* and *MFLSS/GF*. (A) The teeth ranging from the right mandibular first premolar to the last molar were extracted in Beagle dogs. (B) Following tooth extraction, a rectangular defect was generated using both reciprocating and sagittal saws. (C) 3 months post-osteotomy, bone grafting was conducted to address the defect utilizing bone substitutes and membrane application.

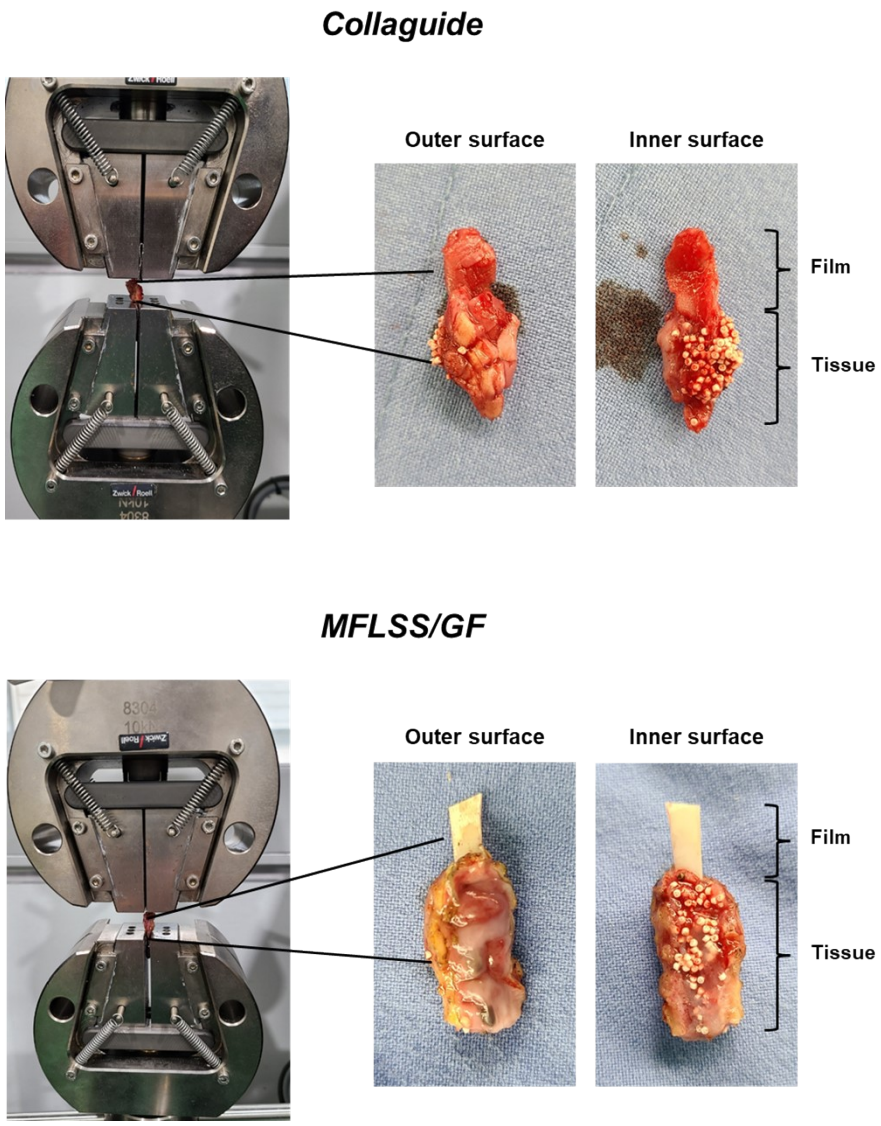

Fig. S5. Mechanical strength analysis (lap-shear test) of film-epithelial adhesion samples (*Collaguide* and *MFLSS*/*GF*).

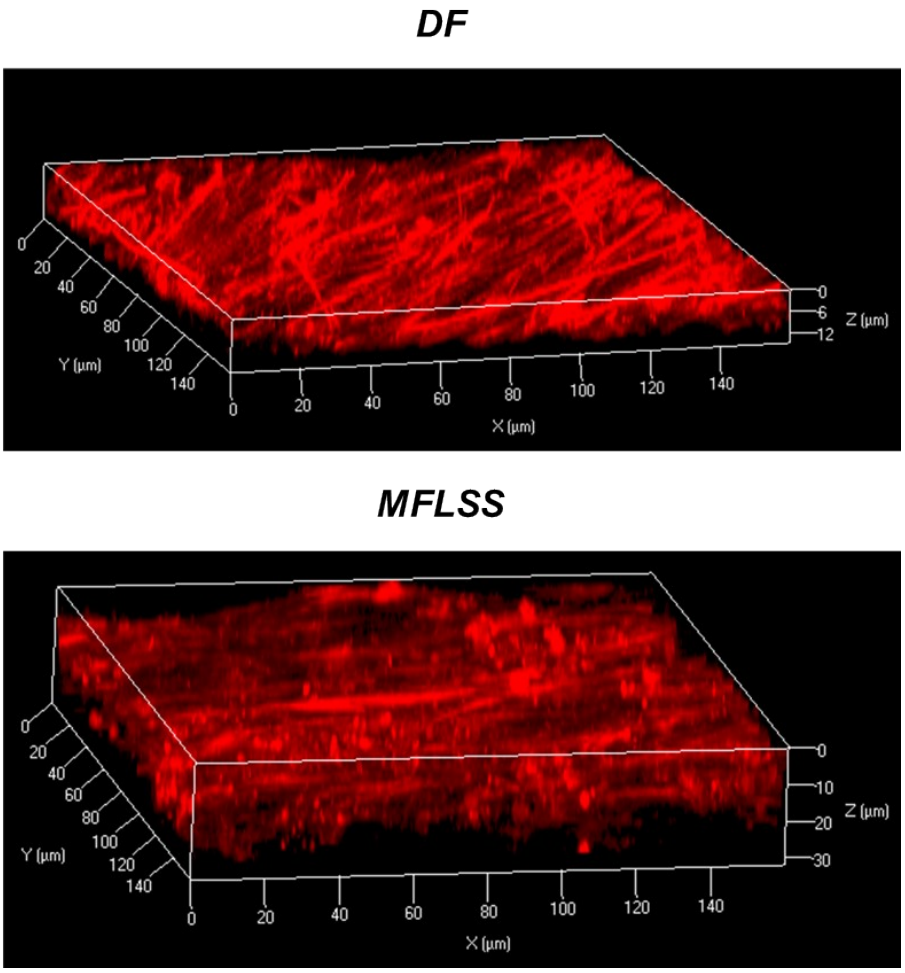

Fig. S6. Confocal microscopy-based three-dimensional visualization of F-actin (red) stained cells cultured on each film (*DF* and *MFLSS*).

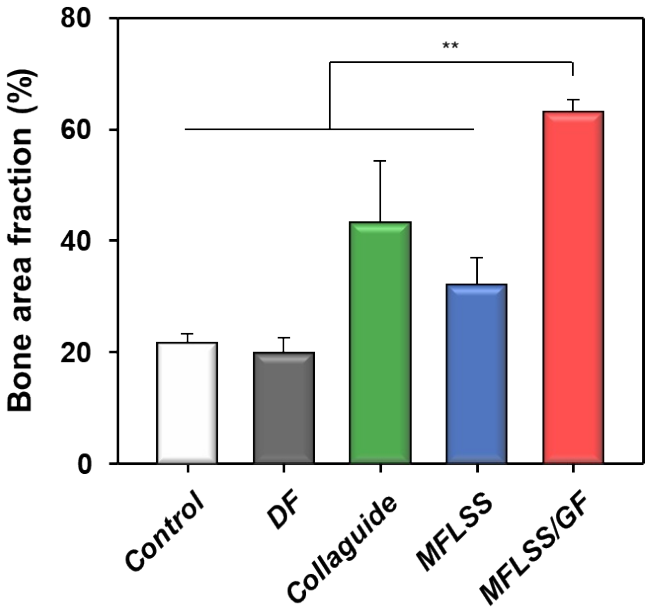

Fig. S7. Quantitative analysis of the new bone area fraction within rat calvarial defects at 8 weeks post-implantation. The bone area fraction was calculated from dorsal micro-CT images as the percentage of mineralized tissue within the predefined defect region of interest (ROI). Data are presented as mean ± SD (n = 3). $^{**}p < 0.01$.

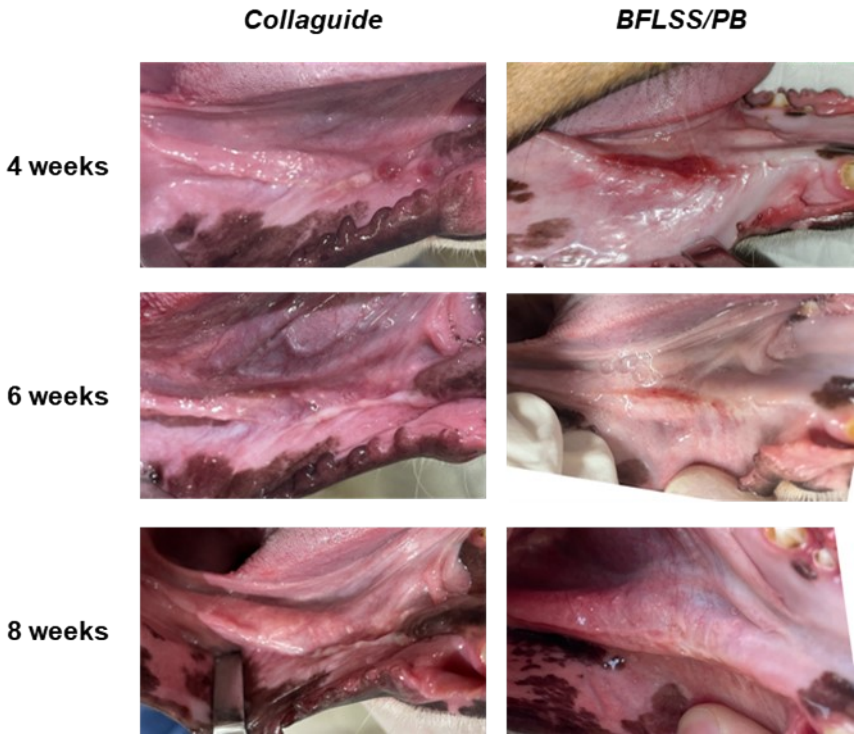

Fig. S8. Representative examples of epithelial healing following bone grafting with bone substitutes, *Collaguide*, and *MFLSS/GF*. Epithelial integrity was maintained without membrane exposure, a critical factor for optimal bone regeneration.